Arabidopsis *Deficient in Cutin Ferulate* Encodes a Transferase Required for Feruloylation of ω-Hydroxy Fatty Acids in Cutin Polyester[1][W][OA]

Carsten Rautengarten, Berit Ebert, Mario Ouellet, Majse Nafisi, Edward E.K. Baidoo, Peter Benke, Maria Stranne, Aindrila Mukhopadhyay, Jay D. Keasling, Yumiko Sakuragi, and Henrik Vibe Scheller*

Feedstocks Division (C.R., B.E., H.V.S.), Fuel Synthesis Division (M.O., E.E.K.B., P.B., J.D.K.), and Technology Division (M.O., A.M.), Joint BioEnergy Institute, Lawrence Berkeley National Laboratory, Emeryville, California 94608; Department of Plant Biology and Biotechnology (M.N., M.S., Y.S.) and Villum Kann Rasmussen (VKR) Research Center ProActive Plants (M.N., M.S., Y.S.), University of Copenhagen, 1870 Frederiksberg, Denmark; and Department of Plant and Microbial Biology, University of California, Berkeley, California 94720 (H.V.S.)

The cuticle is a complex aliphatic polymeric layer connected to the cell wall and covers surfaces of all aerial plant organs. The cuticle prevents nonstomatal water loss, regulates gas exchange, and acts as a barrier against pathogen infection. The cuticle is synthesized by epidermal cells and predominantly consists of an aliphatic polymer matrix (cutin) and intracuticular and epicuticular waxes. Cutin monomers are primarily C_{16} and C_{18} unsubstituted, ω-hydroxy, and α,ω-dicarboxylic fatty acids. Phenolics such as ferulate and *p*-coumarate esters also contribute to a minor extent to the cutin polymer. Here, we present the characterization of a novel acyl-coenzyme A (CoA)-dependent acyl-transferase that is encoded by a gene designated *Deficient in Cutin Ferulate* (*DCF*). The DCF protein is responsible for the feruloylation of ω-hydroxy fatty acids incorporated into the cutin polymer of aerial Arabidopsis (*Arabidopsis thaliana*) organs. The enzyme specifically transfers hydroxycinnamic acids using ω-hydroxy fatty acids as acyl acceptors and hydroxycinnamoyl-CoAs, preferentially feruloyl-CoA and sinapoyl-CoA, as acyl donors in vitro. Arabidopsis mutant lines carrying *DCF* loss-of-function alleles are devoid of rosette leaf cutin ferulate and exhibit a 50% reduction in ferulic acid content in stem insoluble residues. *DCF* is specifically expressed in the epidermis throughout all green Arabidopsis organs. The DCF protein localizes to the cytosol, suggesting that the feruloylation of cutin monomers takes place in the cytoplasm.

The cuticle, a complex polymeric layer connected to the cell wall of epidermal cells, covers the surfaces of all aerial plant organs. The cuticle prevents nonstomatal water loss, regulates gas exchange, acts as a barrier against pathogen infection, and prevents organ fusions (Lolle et al., 1998; Sieber et al., 2000). The plant cuticle is synthesized by epidermal cells and predominantly consists of a lipophilic polymer matrix (cutin) and intracuticular and epicuticular waxes. Cutin monomers are primarily aliphatic C_{16} and C_{18} unsubstituted, ω-hydroxy, and α,ω-dicarboxylic fatty acids. Polyhydroxy fatty acids, fatty alcohols, phenolic acids such as ferulic and *p*-coumaric acid, and glycerol may also contribute to cutin composition in different plant species (Baker and Martin, 1963; Kolattukudy, 1980; Pollard et al., 2008; Samuels et al., 2008; Schreiber, 2010).

In Arabidopsis (*Arabidopsis thaliana*), several enzymes have been identified to be involved in cutin monomer synthesis and polymerization processes, such as glycerol-3-phosphate acyl-transferases 4 and 8 (Li et al., 2007), Bodyguard (Kurdyukov et al., 2006), and Defective in Cuticular Ridges (DCR), a BAHD family enzyme involved in cutin polyester synthesis in Arabidopsis roots, flowers, and seeds. *DCR* mutant lines are characterized by an almost complete lack of 9 (10),16-dihydroxy-hexadecanoic acid, a major component of the flower cutin polymer, accompanied by several cuticle-associated phenotypic alterations in response to abiotic stresses (e.g. impaired salinity and osmotic stress response; Panikashvili et al., 2009). *DCR* encodes a diacylglycerol acyl-transferase that catalyzes the formation of triacylglycerol from diacylglycerol using acyl-CoA as the acyl donor in vitro (Rani et al., 2010).

Recently, another Arabidopsis BAHD family member, Hydroxycinnamoyl-CoA:ω-Hydroxyacid *O*-Hydroxycinnamoyl-Transferase (HHT)/Aliphatic Suberin Feruloyl-Transferase (ASFT), was identified

[1] This work was supported by the U.S. Department of Energy, Office of Science, Office of Biological and Environmental Research (contract no. DE–AC02–05CH11231).

* Corresponding author; e-mail hscheller@lbl.gov.

The author responsible for distribution of materials integral to the findings presented in this article in accordance with the policy described in the Instructions for Authors (www.plantphysiol.org) is: Henrik Vibe Scheller (hscheller@lbl.gov).

[W] The online version of this article contains Web-only data.

[OA] Open Access articles can be viewed online without a subscription.

www.plantphysiol.org/cgi/doi/10.1104/pp.111.187187

and shown to be involved in the acyl-CoA-dependent feruloylation of aliphatic suberin monomers in Arabidopsis roots and seeds. Suberin represents another plant polymer composed of polyesters and aromatics. Compared with cutin, suberin has a more complex monomer composition and is structurally different. Suberin is predominantly found in internal cell walls in underground organs and some other organs (Kolattukudy, 1980). The HHT/ASFT enzyme has been demonstrated to catalyze the synthesis of 16-feruloyl-palmitic acid by the use of feruloyl-CoA as acyl donor and 16-hydroxy-hexadecanoic acid (16-hydroxy-palmitic acid) as acyl acceptor in vitro (Gou et al., 2009; Molina et al., 2009).

In Arabidopsis, the acyl-CoA dependent acyltransferase (BAHD) protein family consists of 55 to 61 members and, based on sequence similarity, can be divided into five distinct clades (Yu et al., 2009). The BAHD family comprises functionally divergent enzymes. The conserved HXXXD and DFGWG motifs are characteristic for almost all family members. So far, most of the characterized enzymes can be categorized into three functional classes: alcohol acetyl-transferases (Dudareva and Pichersky, 2000; D'Auria et al., 2002, 2007a), anthocyanin/flavonoid acyl-transferases (Suzuki et al., 2001; D'Auria et al., 2007b; Luo et al., 2007; Yu et al., 2008; Taguchi et al., 2010), and hydroxycinnamoyl-transferases (Luo et al., 2009; Gou et al., 2009; Molina et al., 2009).

Here, we present the characterization of a novel BAHD family enzyme, Defective in Cutin Feruloylation (DCF), involved in the feruloylation of ω-hydroxy fatty acids incorporated into the cutin polymer of aerial Arabidopsis organs. Mutant lines carrying loss-of-function alleles of *DCF* are devoid of cutin ferulate in rosette leaves and exhibit about 50% reduction in ferulate content in insoluble residues derived from the stem. *DCF* is specifically expressed in epidermal cells throughout all green Arabidopsis organs. The DCF protein localizes to the cytosol, suggesting that the feruloylation of cutin monomers takes place in the cytoplasm. The enzyme transfers hydroxycinnamic acids using ω-hydroxy fatty acids as acyl acceptor and hydroxycinnamate-CoAs as acyl donors in vitro.

RESULTS

Hydroxycinnamate Contents in Arabidopsis Aerial Organs and the Identification of Ferulic Acid-Deficient Mutants

To elucidate the contents of ester-bound hydroxycinnamic acids, specifically ferulic and *p*-coumaric acid, we prepared cell walls from various Arabidopsis aerial organs. Saponification and ethyl acetate extraction of total cell wall preparations and subsequent HPLC analysis revealed the highest ferulic and *p*-coumaric acid contents in fully expanded rosette leaves derived from vegetative stage plants (46 ± 2 and 27 ± 2 nmol g^{-1} dry residue) and top parts of inflorescence stems (54 ± 1 and 57 ± 1 nmol g^{-1} dry residue). Lower ferulic and *p*-coumaric acid amounts were released from extracts derived from middle (39 ± 1 and 29 ± 1 nmol g^{-1} dry residue) and bottom (39 ± 1 and 25 ± 1 nmol g^{-1} dry residue) parts of inflorescence stems and leaves of reproductive stage plants (20 ± 1 and 37 ± 1 nmol g^{-1} dry residue; Table I).

Hitherto, all characterized plant hydroxycinnamoyl-transferases belonged to the HXXXD-type acyltransferase (BAHD family) gene family. To identify the Arabidopsis hydroxycinnamoyl-transferases responsible for the incorporation of ferulic and *p*-coumaric acid into the plant cell wall, we performed a systematic screen of T-DNA insertion lines in BAHD family-encoding genes for a reduction in ferulic acid or *p*-coumaric acid contents in leaf cell wall preparations. Consequently, two mutant lines comprising independent T-DNA insertions in the same genetic locus (At3g48720) were identified with strongly reduced ferulic acid release from rosette leaf extracts, whereas *p*-coumaric acid amounts were substantially unaltered compared with wild-type plants. Based on a subsequent detailed characterization, the gene was named *DCF*.

Loss of *DCF* Expression Results in Ferulate Deficiency of Arabidopsis Cell Walls

The two *DCF* mutant alleles, *dcf-1* (Salk_040807) and *dcf-2* (Sail_513_C03), carrying a T-DNA insertion either in the second exon or the only intron were identified in

Table I. *Hydroxycinnamate contents (nmol g^{-1} dry weight) in different Arabidopsis organs and developmental stages of the Col-0 wild type, dcf-1, and three independent complemented dcf-1 mutant lines (DCF_{pro}:DCF-HA/dcf-1)*

Data represent means ± SD of three biological replicates. FA, Ferulic acid; FS, flowering stage; *p*-CA, *p*-coumaric acid; VS, vegetative stage. Asterisks indicate significance as follows: * 5% level, ** 1% level, and *** 0.1% level.

Organ and Stage	Col-0		*dcf-1*		DCF_{pro}:DCF-HA / *dcf-1*					
					Line 11		Line 14		Line 15	
	FA	*p*-CA	FA	*p*-CA	FA	*p*-CA	FA	*p*-CA	FA	*p*-CA
Leaf VS	46 ± 2	27 ± 2	5 ± 1***	23 ± 3	208 ± 4***	28 ± 2	101 ± 3***	25 ± 2	144 ± 7***	27 ± 1
Leaf FS	20 ± 1	37 ± 1	12 ± 1**	39 ± 2	76 ± 4**	35 ± 3	90 ± 5**	39 ± 2	67 ± 3**	47 ± 1**
Stem bottom	39 ± 1	25 ± 1	20 ± 2**	20 ± 5	49 ± 1**	42 ± 2**	55 ± 1**	29 ± 2	46 ± 1**	27 ± 2
Stem middle	39 ± 1	29 ± 1	19 ± 1**	28 ± 1	63 ± 2**	51 ± 2**	72 ± 3**	38 ± 1*	57 ± 2**	31 ± 3
Stem top	54 ± 1	57 ± 1	23 ± 1***	57 ± 3	111 ± 2***	81 ± 5**	109 ± 1***	77 ± 2**	102 ± 2***	77 ± 1**

the SIGnAL (Alonso et al., 2003) and Syngenta (McElver et al., 2001) collections. Plants carrying homozygous insertions were identified by PCR. The effects of the T-DNA insertions on mRNA expression levels were examined using reverse transcription (RT)-PCR. No *DCF* transcripts were detected in homozygous *dcf-1* and *dcf-2* individuals, which is indicative of a loss of function of the *DCF* gene in the corresponding mutant lines (Fig. 1A).

None of the mutant lines showed any morphological and developmental phenotypic alterations under standard growth conditions compared with ecotype Columbia (Col-0) wild-type plants and *quartet1* (*qrt1*) (genetic background line for *dcf-2*). However, ferulic acid contents in total cell wall hydrolysates from rosette leaves of vegetative stage plants were significantly ($P < 0.01$) reduced to 11% and 12% of the wild-type level in *dcf-1* and *dcf-2*, respectively (Fig. 1B; Table I). In inflorescence stems and rosette leaves of reproductive stage plants, significant reductions of 40% to 60% in ferulic acid contents were observed (Fig. 1B; Table I). In contrast, *p*-coumaric acid, the second predominant hydroxycinnamic acid detected by HPLC, was only slightly reduced, by 15% ($P < 0.13$), in rosette leaf extracts of vegetative stage plants and was unaltered in cell wall preparations derived from Arabidopsis organs of reproductive stage plants (Fig. 1B).

Ferulate Deficiency in *dcf* Mutants Affects the Cutin Polyester

To determine the cell wall component affected by ferulic acid deficiency, we sequentially extracted extensively delipidated insoluble cell wall residues with cyclohexane diamine tetraacetic acid (CDTA) and sodium carbonate solutions to release pectins. This was followed by endo-β-xylanase treatment to release xylans and driselase to release the remaining cell wall sugars. The corresponding fractions we hydrolyzed separately, and in agreement with Gou et al. (2009), we did not detect significant amounts of ferulic or *p*-coumaric acid released in any of those hydrolysates. Only saponification or depolymerization of the remaining insoluble residue released ferulic and *p*-coumaric acid or their methyl derivatives, respectively. Consistent with this observation, no significant differences in ferulic acid and *p*-coumaric acid release were observed when comparing acid-catalyzed depolymerization of carbohydrate-free residues with base hydrolysis of total cell wall residues (Fig. 2). Taken together, these results strongly indicate that the insoluble cutin polymer is the only source of esterified ferulic and *p*-coumaric acids in Arabidopsis leaf tissue. In Arabidopsis stems undergoing secondary growth, hydroxycinnamoyl esters of suberin may also contribute to this pool.

In delipidated, carbohydrate-free cell wall residues from Col-0 and *qrt1*, two major peaks were apparent upon acid-catalyzed depolymerization and subsequent HPLC analysis (Fig. 1C). Liquid chromatography-atmospheric pressure chemical ionization-mass spectrometry (LC-APCI-MS) identified compound A with a parent ion mass $[M-H]^-$ of 177.01 (mass-to-charge ratio [*m/z*]), consistent with the molecular mass of methyl-*p*-coumarate, and the predominant compound B with a molecular ion $[M-H]^-$ of 207.07 (*m/z*) and $[M+H]^+$ of 209.08 (*m/z*), consistent with the molecular mass of the methyl-ester derivative of ferulate. Additional diagnostic ions with $[M+H]^+$ of 177.05 (*m/z*) and 149.06 (*m/z*) are indicative of a loss of a methoxy group and a loss of a carbonyl group, respectively (Fig. 1D). In contrast to the wild type, in leaf extracts derived from

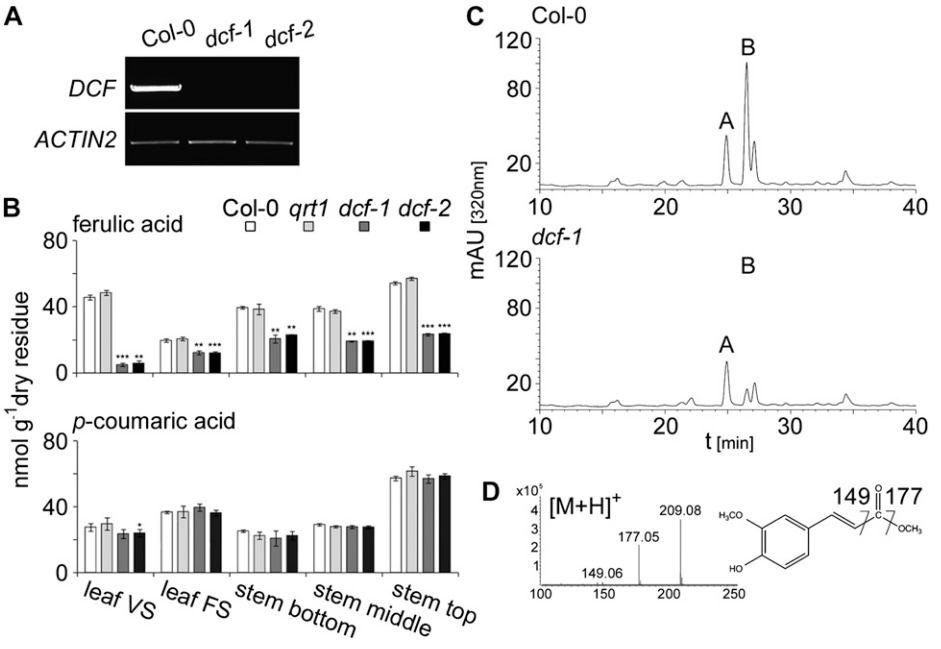

Figure 1. Identification and biochemical characterization of *DCF* mutant lines. A, RT-PCR analysis of *DCF* gene expression in *dcf-1* and *dcf-2* mutants. B, Ferulic- and *p*-coumaric acid contents of leaf and stem tissue of *dcf* mutants compared with the Col-0 and *qrt1* wild types. Values represent means ± SD of at least three biological replicates. Significant differences between mutant and parental lines are indicated (Student's *t* test; *** $P < 0.001$, ** $P < 0.01$, * $P < 0.05$). FS, Flowering stage; VS, vegetative stage. C, Representative HPLC profiles of phenolics released upon depolymerization of wild-type (Col-0) and *dcf* mutant derived delipidated residues. mAU, Milliabsorbance units. D, Mass spectrum and chemical structure of compound B corresponding to methyl-ferulate.

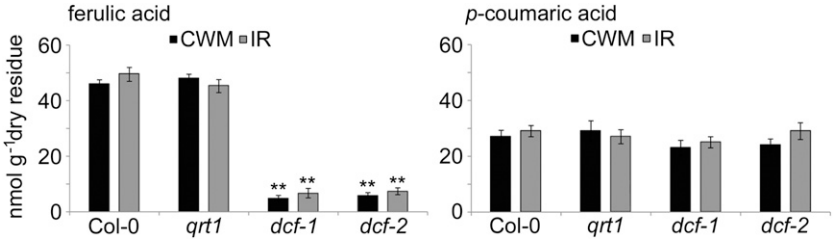

Figure 2. Ferulic- and *p*-coumaric acid amounts released upon base hydrolysis of total cell wall (CWM) preparations and acid-catalyzed depolymerization of delipidated, carbohydrate-free insoluble residues (IR). Values represent means ± SD of at least three biological replicates. Significant differences between mutant and parental lines are indicated (Student's *t* test; ** $P < 0.01$).

dcf-1 and *dcf-2* mutants, the methyl-ferulate peak was barely detected, whereas the corresponding methyl-*p*-coumarate peak was essentially unchanged (Fig. 1C).

To investigate the effect of the lack of ferulate in *dcf* mutants on cutin lipid monomer composition, we analyzed delipidated extractive-free residues after acid-catalyzed depolymerization using gas chromatography-mass spectrometry (GC-MS). Except for the expected absence of the methyl-ferulate peak in *dcf* mutants, GC-MS analyses of lipid monomers revealed a slight increase in saturated and monounsaturated α,ω-dicarboxylic acid contents in *dcf* mutants compared with the respective background lines and a corresponding slight decrease in 16:0 fatty acids (Fig. 3). The content of 16:0 ω-hydroxy acids was unchanged (Fig. 3). Despite the slight alterations in lipid monomer composition, these data suggest that the DCF protein predominantly functions in ferulic acid incorporation into the cutin polymer.

DCF Expression Is Restricted to the Epidermis of Aerial Organs

The expression patterns of *DCF* in various tissues such as roots, seedlings, and rosette leaves, different parts of inflorescence stems, inflorescences, and siliques at different developmental stages were assessed by quantitative (q)RT-PCR. *DCF* transcripts were exclusively detected in green tissues, with the highest amounts in the upper part of inflorescence stems. Strong expression was apparent in 10-d-old seedlings, expanding and mature rosette leaves (Fig. 4A), inflorescences, and siliques at 4 to 6 d post anthesis (DPA). Lower expression levels were detected in middle and bottom parts of inflorescence stems and in siliques containing seeds at 6 to 8 DPA. Almost no transcripts were detected in maturing siliques at 8 to 12 DPA, and no expression was detected in root tissue (Fig. 4A).

To gain better spatially and developmentally resolved information on *DCF* expression, we stably expressed a translational fusion protein carrying a C-terminal yellow fluorescent protein (YFP) tag driven by the *DCF* promoter in Arabidopsis. Consistent with the qRT-PCR data, the DCF-YFP protein was only detected in green tissue such as stem and leaf but not in root. In plants at the vegetative stage, DCF-YFP was predominantly expressed in the cotyledons of 10-d-old seedlings as well as in expanding (approximately 50% of final size) and mature leaves (Fig. 4B). Only

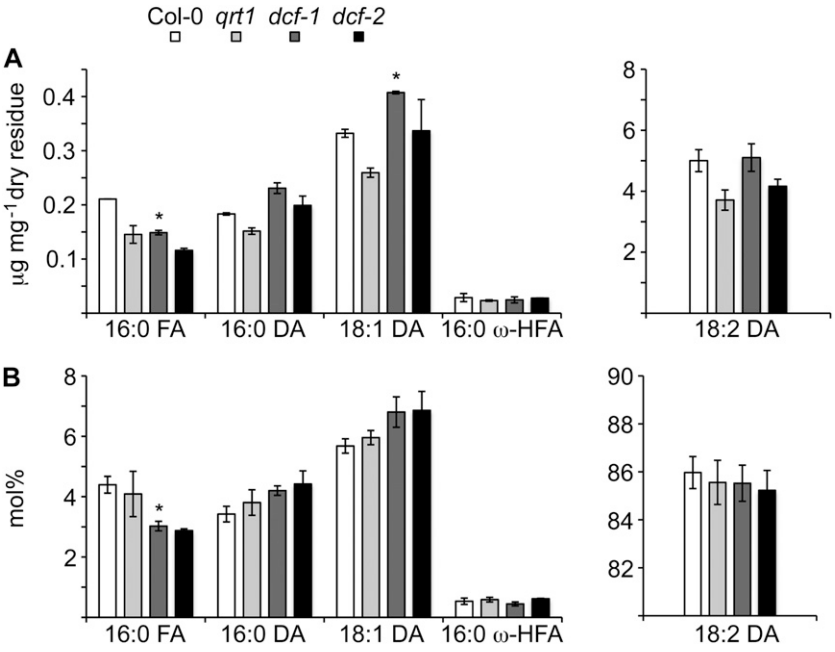

Figure 3. Lipidic polyester monomer composition of wild-type and *dcf* mutant leaves. Delipidated residues were depolymerized with methanolic hydrochloric acid, and released monomers were analyzed by GC-MS. Values represent means ± SD of at least three biological replicates. Significant differences between mutant and parental lines are indicated (Student's *t* test; * $P < 0.05$).

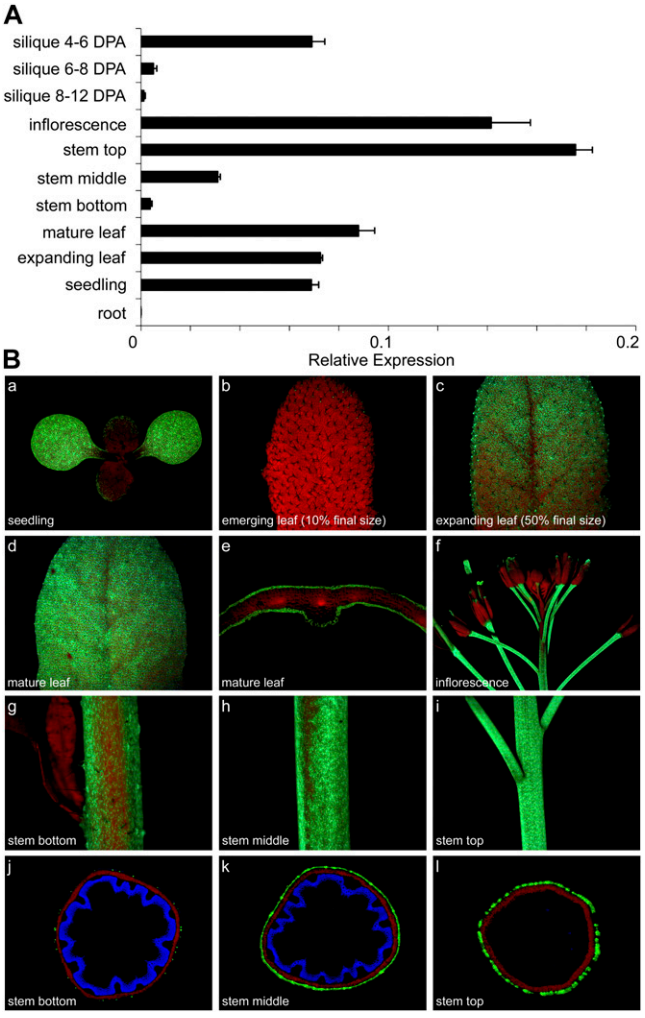

Figure 4. *DCF* expression in major Arabidopsis organs and at different developmental stages. A, qRT-PCR analysis. Seedlings were grown for 10 d in sterile culture. Leaves were harvested from 5-week-old plants (rosette stage). Other material was derived from 8-week-old flowering plants. Stems were divided into three parts, and siliques were harvested at the indicated time points. The levels of expression are calculated relative to the *UBQ10* gene, and values represent means ± SD of three biological replicates. B, DCF_{pro}:*DCF-YFP* expression pattern in transgenic Arabidopsis plants. DCF was stably expressed in Arabidopsis as a C-terminal translational YFP fusion protein under the control of the native promoter. YFP fluorescence is displayed in green (a–l), and autofluorescence of stem sections upon UV light excitation is displayed in blue (j–l).

low YFP signals were apparent in emerging rosette leaves (approximately 10% of final size). During the reproductive stage, expression was apparent in inflorescence stems, which continuously decreased from top to bottom, developing siliques, and flower pedicels (Fig. 4B). Cross-sections through different parts of inflorescence stems and mature rosette leaves revealed an epidermis-specific expression pattern of the DCF protein, indicating a function in cuticle synthesis and development (Fig. 4B).

Our results obtained by qRT-PCR and analysis of DCF_{pro}:*DCF-YFP*-expressing plants are substantially supported by microarray hybridization data, which suggest exclusive *DCF* expression in aboveground organs as well as epidermis-specific expression in upper parts of Arabidopsis inflorescence stems (Schmid et al., 2005; Suh et al., 2005; Winter et al., 2007).

DCF Is a Cytosolic Protein

The DCF protein is predicted not to possess any transmembrane domain or known targeting sequence (Yu et al., 2009). To experimentally investigate the subcellular localization of DCF, we analyzed DCF-YFP fusions stably expressed and driven by the native *DCF* promoter in Arabidopsis. As shown in Figure 5A, in DCF_{pro}:*DCF-YFP*-expressing plants, YFP signals originated from all over the cell, indicative of a cytosolic localization. Strong YFP signals were also observed possibly originating from cell walls, plasma membrane, or the intercellular space. However, plasmolysis experiments (Fig. 5B) and protein subcellular fractionations (see below) contradict this possibility.

To confirm our results on DCF-YFP subcellular localization, we separated plant protein extracts derived from transgenic Arabidopsis lines expressing the DCF protein with a C-terminal hemagglutinin (HA) tag driven by its native promoter into cytosolic and microsomal fractions. As shown in Figure 5C, DCF was detected in the cytosolic fraction, and almost no signals were observed in the microsomal fraction predominantly containing mitochondria- and Golgi-

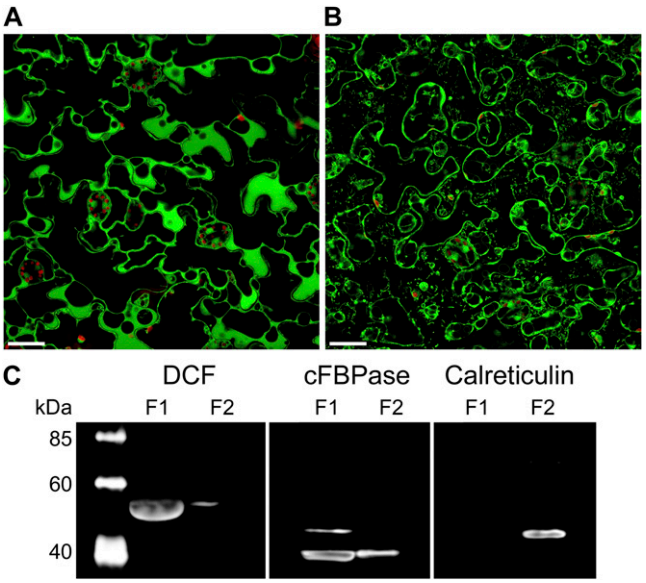

Figure 5. Subcellular localization of the DCF protein. A and B, Single-plane confocal micrographs of leaf epidermis of DCF_{pro}:*DCF-YFP*-expressing transgenic plants (A) and after plasmolysis (B). Bars = 25 μm. C, Subcellular fractionation of protein samples derived from DCF_{pro}:*DCF-HA*-expressing transgenic plants. F1, Cytosolic fraction; F2, detergent-solubilized microsomal fraction.

localized as well as membrane proteins. As a control, we used an antibody raised against Arabidopsis cytosolic fructose-1,6-bisphosphatase (cFBPase [cytosolic protein]; Strand et al., 2000), which detects two cFBPase isoforms with molecular masses of 45 and 37 kD. The 37-kD cFBPase isoform was also present in the microsomal fraction, probably due to its high abundance. Calreticulin (CRT) as endoplasmic reticulum resident protein (Jia et al., 2009; Christensen et al., 2010) was exclusively detected with an anti-CRT antibody in the microsomal fraction with a molecular mass between 40 and 60 kD, consistent with the mass of Arabidopsis CRTs of about 48 kD. In conclusion, the lack of any known targeting sequence, our data obtained from DCF_{pro}:*DCF-YFP* localization, as well as subcellular protein fractionations on DCF_{pro}:*DCF-HA*-expressing plants provide strong evidence for a cytosolic localization of the DCF protein.

Recombinant DCF Functions as a Hydroxycinnamoyl-CoA: ω-Hydroxy Fatty Acid Transferase

To establish its enzymatic characteristics, we heterologously expressed DCF as an N-terminal 6× His tag fusion protein in *Escherichia coli*. SDS-PAGE and immunoblot analysis of the affinity-purified protein revealed a predominant band of about 50 kD detected by Coomassie blue staining and by an anti-His antibody (Fig. 6A), which is in agreement with the predicted molecular mass of 48.0 kD (plus an N-terminal His tag of 2.6 kD).

The recombinant protein was tested for hydroxycinnamoyl-CoA-transferase activity using feruloyl-CoA as acyl donor. As acyl acceptor, we provided 16-hydroxy-palmitic acid, the major ω-hydroxy fatty acid incorporated into Arabidopsis cutin. The reaction products were analyzed by LC-APCI-MS and revealed a major product with a UV absorption spectrum similar to ferulic acid and a major molecular ion of 449.28 $[M+H]^+$, which is consistent with the single positively charged molecular mass of 16-feruloyl-palmitic acid of 449.28 D. Additional diagnostic fragment ions of m/z = 177.05 $[feruloyl]^+$ and m/z = 209.08 [ferulic acid methyl ester]$^+$ further confirmed the existence of a feruloyl residue in the identified compound (Fig. 6, D and E). A side product, methyl-ferulate, was detected resulting from the reactivity of DCF with methanol, the solvent we used for 16-hydroxy-palmitic acid in our transferase reaction setup. No similar products were detected in control reactions containing the heat-inactivated recombinant enzyme (Fig. 6C).

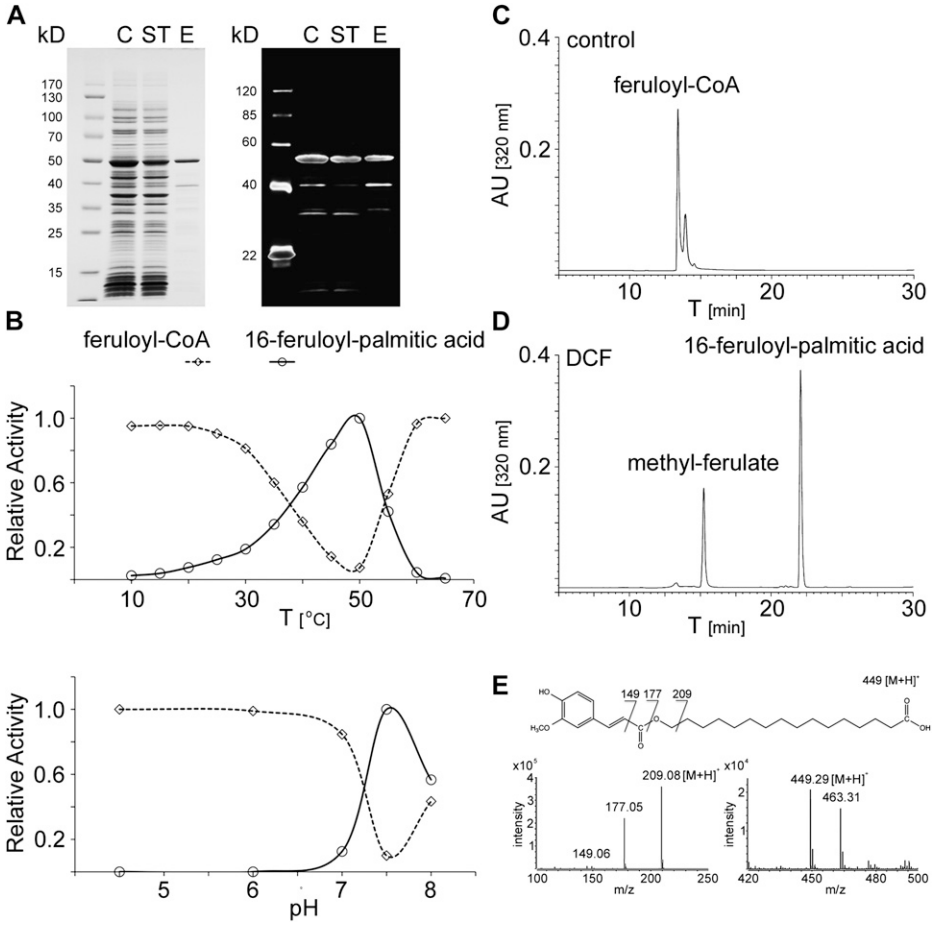

Figure 6. In vitro hydroxycinnamoyl-CoA transferase activity of recombinant DCF protein. A, SDS-PAGE of purified recombinant DCF protein stained with Coomassie Brilliant Blue and corresponding immunoblot analysis. C, Crude extract; ST, supernatant; E, eluate. B, Temperature and pH profiles of recombinant DCF feruloyl-transferase activity. C and D, HPLC chromatograms of products formed after the reaction of recombinant DCF (D) and control reaction with heat-inactivated enzyme (C) with feruloyl-CoA as acyl donor and 16-hydroxy-palmitic acid as acyl acceptor. AU, Absorbance units. E, Mass spectra and chemical structures of the reaction products, ferulic acid methyl-ester and 16-feruloyl-palmitic acid.

Temperature and pH profiles revealed that the DCF enzyme was most active at 50°C and at a pH of 7.5 (Fig. 6B). Whereas the addition of monovalent cations (Na^+, K^+, Li^+) had no effect on enzymatic activity, the addition of divalent cations (Mg^{2+}, Mn^{2+}, Zn^{2+}, Cu^{2+}, Ni^{2+}, Ba^{2+}, Ca^{2+}) almost completely inhibited the transferase reaction at 2 mM concentration. The highest feruloyl-transferase activity was observed with ω-hydroxy fatty acids as acyl acceptors, with $C_{16} > C_{17} > C_{15}$. Only negligible activity was observed with longer chain (C_{20} and C_{22}) ω-hydroxy fatty acids (Table II). Short-chain primary alcohols were also used as acceptors, but also with only minor activities. No activity was observed with fatty acids lacking an ω-hydroxy group, amines, monolignols, and shikimic acid (Table II).

Besides feruloyl-CoA, the enzyme was also active with all other naturally occurring hydroxycinnamate-CoAs provided as acyl donors. The affinity of the DCF protein for 16-hydroxy-palmitic acid when using sinapoyl-CoA as acyl donor (K_m = 173 μM) was even higher than that observed when providing feruloyl-CoA as acyl donor (K_m = 362 μM). Considerably lower catalytic activities were apparent with caffeoyl-CoA and *p*-coumaroyl-CoA (Table III).

The determination of in vivo feruloyl-transferase activities in crude cytosolic leaf protein extracts using feruloyl-CoA as acyl donor and 16-hydroxy-palmitic acid as acceptor revealed almost no activity in *dcf-1* (0.5%) and *dcf-2* (0.6%) mutants compared with the respective wild types with corresponding activities set to 100% (Table IV).

Introduction of a Functional *DCF* Restores the Mutant Biochemical Phenotype

To investigate whether the introduction of a functional *DCF* gene restores the biochemical *dcf* mutant phenotype, we transformed *dcf-1* mutants with a construct (*DCF_{pro}:DCF-HA*) expressing the DCF protein as a HA tag fusion under the control of the native *DCF* promoter. Transgenic lines were selected and analyzed for DCF expression by immunoblotting. Three independent lines revealing strong expression of the DCF protein were analyzed for ferulic acid content. As shown in Table I, ferulic acid contents in hydrolyzed

Table II. *In vitro substrate specificities of the recombinant DCF protein*

Relative activities are given in percentage activity with feruloyl-CoA and 16-hydroxy-hexadecanoic acid. n.d., Not detected.

Substance	Activity	K_m	V_{max}
	%	M	*pmol mg^{-1} min^{-1}*
Acyl acceptor[a]			
15-Hydroxy-pentadecanoic acid	51	–	–
16-Hydroxy-hexadecanoic acid	100	36.22 ± 2.64 (×10^{-5})[a]	3.78 ± 0.12[a]
		17.27 ± 1.11 (×10^{-5})[b]	4.15 ± 0.09[b]
17-Hydroxy-heptadecanoic acid	91	–	–
20-Hydroxy-eicosanoic acid	5	–	–
22-Hydroxy-docosanoic acid	0.1	–	–
12-Hydroxy-octadecanoic acid	n.d.	–	–
Methanol	1	–	–
Ethanol	1	–	–
1-Propanol	6	–	–
2-Propanol	n.d.	–	–
1-Butanol	17	–	–
1-Hexanol	3	–	–
1-Octanol	n.d.	–	–
1-Dodecanol	n.d.	–	–
1-Tetradecanol	n.d.	–	–
1-Hexadecanol	n.d.	–	–
1-Octadecanol	n.d.	–	–
2-Hexenol	n.d.	–	–
Dodecanedioic acid	n.d.	–	–
Hexadecanedioic acid	n.d.	–	–
Hexadecanoic acid methyl ester	n.d.	–	–
Hexadecane	n.d.	–	–
Lignoceric acid	n.d.	–	–
Coniferyl alcohol	n.d.	–	–
Shikimic acid	n.d.	–	–
Tyramine	n.d.	–	–
Tryptamine	n.d.	–	–

[a]Feruloyl-CoA as acyl donor. [b]Sinapoyl-CoA as acyl donor.

Table III. *Relative in vitro activities of the recombinant DCF protein with different hydroxycinnamate-CoAs as acyl donors and 16-hydroxy-palmitic acid as acyl acceptor*

Acyl Donor	Activity
	%
Feruloyl-CoA	100
Sinapoyl-CoA	169
Caffeoyl-CoA	22
p-Coumaroyl-CoA	9

extractive-free residues were not only restored to the wild-type level but were up to five times higher with correspondingly elevated feruloyl-transferase activities in crude leaf protein extracts (Table IV). These results further support the identity of DCF as a feruloyl-transferase and that a dysfunctional *DCF* in the *dcf* mutants is responsible for the reductions in ferulic acid contents in the cutin polymer.

DISCUSSION

In previous studies, ferulic acid has been established as the major aromatic constituent of Arabidopsis root and seed suberin involved in controlling ion uptake. Mutant lines defective in a BAHD family gene, *HHT* (alias *ASFT*), were shown to be almost devoid of root and seed suberin ferulate, resulting in an increased permeability of seed coats and root meristems to salts. The corresponding enzyme was proven to transfer ferulate from feruloyl-CoA to ω-hydroxy fatty acids, specifically 16-hydroxy-palmitic acid, in vitro (Gou et al., 2009; Molina et al., 2009).

Despite certain significant structural differences, suberin and cutin both consist of a polyaliphatic domain predominantly composed of fatty acids, ω-hydroxy fatty acids, primary alcohols, and α,ω-dicarboxylic acids. Suberin also contains a polyaromatic domain consisting of C-C and ether-linked ferulate, *p*-coumarate, and sinapate, most likely cross-linking the aliphatic domain to cell wall polysaccharides (Kolattukudy, 1980, 2001; Franke et al., 2005; Pollard et al., 2008; Ranathunge et al., 2011). In contrast to cutin, which is part of the cuticle covering the epidermis of aerial plant organs, suberin is primarily deposited on the inner face of primary cell walls in underground tissues like roots, in mature seed coats, and in aerial tissues that undergo secondary thickening (Kolattukudy, 1980; Pollard et al., 2008; Ranathunge et al., 2011).

In suberin, aromatic hydroxycinnamyl esters typically constitute about 1% of the total monomers, whereas only a minor contribution of hydroxycinnamyl esters has been assumed for the cutin polymer (Pollard et al., 2008). Indeed, in our studies, the average ferulic acid content in leaf and stem cell wall preparations was about 20 and four times lower compared with highly suberized roots and seeds, respectively (Gou et al., 2009; Molina et al., 2009). However, our calculated total wall-bound ferulic acid amounts of approximately 50 nmol g^{-1} dry weight present in Arabidopsis stems are consistent with a study performed by Gou et al. (2009). In *dcf* mutants, we observed reductions of approximately 90% in ferulic acid content in essentially nonsuberized leaf tissue. In stems, only about a 50% reduction in wall-bound ferulate was evident. Gou et al. (2009) reported that *hht/asft* mutant stems exhibited a similar reduction of about 50% in ferulate content. This might result from essentially nonferuloylated suberin, and our results would argue that the remaining 50% originated from feruloylated cutin. However, to date, there is no histological or chemical evidence for the occurrence of suberin in Arabidopsis inflorescence stems. Thus, HHT/ASFT and DCF may also act redundantly in stem lipidic polymer feruloylation. Further studies have to be performed in order to determine whether both enzymes are expressed in the same tissue or if there might be a diffuse suberin in stems undergoing secondary growth that has been overlooked up to now.

Loss of *DCF* Function Does Not Affect Cutin Lipid Monomer Composition, Cuticle Permeability, and Susceptibility to Pathogens

In our *dcf* mutants, the lack of cutin ferulate was accompanied by slightly elevated levels of saturated and monounsaturated α-ω-dicarboxylic acids, the major lipid monomers of Arabidopsis cutin (Schreiber, 2010). A similar increase in dicarboxylic acids was also observed for *hht/asft* mutants defective in suberin ferulate (Gou et al., 2009). The authors speculate that this might result from the increased availability of the precursor, the ω-hydroxy fatty acids, which also seems to apply to our cutin ferulate-deficient mutants. The primary function suggested for the cuticle is to prevent nonstomatal water loss. Although *dcf* knockout mutants exhibit an almost complete loss in rosette leaf wall-bound ferulic acid, the plants displayed no obvious alteration with respect to the permeability of the cuticle as examined by toluidine blue absorption (data

Table IV. *Feruloyl-transferase activities in leaf cytosolic protein extracts derived from the Col-0 and qrt1 wild type, dcf mutants, and two independent lines expressing DCF as HA tag fusion proteins in the dcf-1 mutant background (DCF_{pro}:DCF-HA/dcf-1)*

Transferase activities were measured with feruloyl-CoA as acyl donor and 16-hydroxy-palmitic acid as acyl acceptor. Data represent means ± SD of three biological replicates. Asterisks indicate significance (*** $P < 0.001$).

Sample	Relative Activity
	% of wild type
Col-0	100 ± 5
dcf-1	0.5 ± 0.1***
qrt1	100 ± 6
dcf-2	0.6 ± 0.2***
DCF_{pro}:DCF-HA/*dcf-1* line 11	508 ± 12***
DCF_{pro}:DCF-HA/*dcf-1* line 15	469 ± 9***

not shown) and chlorophyll extraction assays (Supplemental Fig. S1), suggesting that cutin-bound ferulate does not affect structural and sealing properties of the cuticle in Arabidopsis.

A second important function of the cuticle is to be a protective barrier against pathogen infection (Reina-Pinto and Yephremov, 2009). Arabidopsis mutants with cuticle defects were demonstrated to be resistant to pathogens like the necrotrophic fungus *Botrytis cinerea* (Bessire et al., 2007). However, we did not observe any significantly altered response of *dcf* mutants against *B. cinerea* or the bacterial plant pathogen *Pseudomonas syringae* (Supplemental Fig. S2), which likely might be explained by the unaltered cuticle permeability. We also did not observe any differences in the feeding behavior of herbivores like larvae of the small cabbage butterfly (*Pieris rapae*) or adult flea beetles (*Phyllotreta nemorum*; Supplemental Fig. S3). Taken together, these data suggest that ester-bound ferulate in cutin does not play a significant role in conferring physiological functions, as reported for suberin (Gou et al., 2009).

DCF Is a Hydroxycinnamoyl-CoA:ω-Hydroxy Fatty Acid Transferase

The presence of feruloyl-transferases that transfer ferulate from feruloyl-CoA, as the acyl donor, to ω-hydroxy fatty acids, as acyl acceptors, has been reported for several plant species, such as potato (*Solanum tuberosum*; Lotfy et al., 1994), tobacco (*Nicotiana tabacum*; Lotfy et al., 1996), and, most recently, Arabidopsis (Gou et al., 2009; Molina et al., 2009). Enzymatic activity assays of the recombinant DCF protein revealed similar activity for DCF as for hydroxycinnamoyl-transferase, with a preference for 16-hydroxy-palmitic acid as acyl acceptor and sinapoyl-CoA and feruloyl-CoA as acyl donors. Lower activity was observed with C_{15} and C_{17} ω-hydroxy fatty acids. However, ω-hydroxy acids with an odd number of carbon atoms have not been detected in Arabidopsis cutin and suberin (Franke et al., 2005) and therefore are unlikely substrates for the DCF protein in vivo. In our experiments, longer chain ω-hydroxy fatty acids (C_{20}, C_{22}) were not used or were not used or were used with negligible activity as substrates. Whereas 20 hydroxy-eicosanoic and 22-hydroxy-docosanoic acids have not been detected in Arabidopsis leaf cutin, they constitute, together with 16-hydroxy-palmitic acid, the major ω-hydroxy fatty acid monomers in Arabidopsis root suberin (Franke et al., 2005). Thus, it would be interesting to determine if the longer hydroxy fatty acids are substrates for HHT/ASFT or if only the promoter specificities of *DCF* and *HHT/ASFT* determine their specific functions in cutin or suberin synthesis.

DCF and HHT/ASFT are 60% identical in their amino acid sequences and share several common motifs, including the HXXXD motif, located at the active site of BAHD enzymes, and the structural C-terminal DFGWG motif (Ma et al., 2005; Supplemental Fig. S4). The catalytic properties of the recombinant DCF protein are similar to the reported HHT/ASFT activities (Gou et al., 2009), except that DCF has a higher optimal temperature (50°C). This might emphasize its specific function within epidermal tissues of aboveground organs exposed to direct sunlight and the concomitant elevated temperatures in those tissues. Besides ferulate, we identified *p*-coumarate as the second predominant hydroxycinnamic acid esterified to aliphatic cutin monomers, similar to previously obtained results on suberin (Gou et al., 2009; Molina et al., 2009). Although HHT/ASFT and DCF were also active with *p*-coumaroyl-CoA as acyl donor in vitro, in both *hht/asft* and *dcf* mutants, the *p*-coumaric acid contents in suberin and cutin, respectively, were essentially unaltered. These data suggest a high specificity of HHT/ASFT and DCF for feruloyl-CoA as acyl donor in vivo and lead to the conclusion that there must be another hydroxycinnamoyl-transferase responsible for *p*-coumarate transfer to suberin and cutin monomers in Arabidopsis. However, so far, we did not identify any *p*-coumarate-deficient mutants of BAHD family members within the *DCF* and *HHT/ASFT* clade (Supplemental Fig. S5).

The presence of a feruloyl-transferase activity in Arabidopsis wild-type leaf protein extracts under exogenous supply of feruloyl-CoA, as the acyl donor, and 16-hydroxy-palmitic acid, as the acyl acceptor, and the absence of such activity in *dcf* mutant extracts strongly substantiate the function of DCF as hydroxycinnamoyl-CoA:ω-hydroxy fatty acid transferase.

CONCLUSION

We identified and characterized a mutant almost devoid of ferulic acid in cutin polymers of Arabidopsis leaves. The corresponding gene, *DCF*, belongs to the BAHD superfamily. DCF expression is restricted to the epidermis of aerial organs, the place of cutin synthesis, and localized to the cytosol. We demonstrated that recombinant DCF acts as a hydroxycinnamoyl-CoA:ω-hydroxy fatty acid transferase. The preferred acyl donors of DCF were sinapoyl-CoA and feruloyl-CoA, whereas 16:0 ω-hydroxy fatty acid was the predominant acyl acceptor.

MATERIALS AND METHODS

Chemicals

If not otherwise indicated, chemicals were purchased from Sigma-Aldrich. 17-Hydroxy-heptadecanoic, 20-hydroxy-eicosanoic, and 22-hydroxy-docosanoic acids were purchased from Matreya. Hydroxycinnamate-CoAs were prepared as described previously (Rautengarten et al., 2010).

Sequence Analysis

Amino acid sequences were retrieved using the BLAST algorithm (Altschul et al., 1990) at The Arabidopsis Information Resource (http://www.arabidopsis.org). Deduced amino acid sequences were aligned using the ClustalX program (Thompson et al., 1997) with the default parameter. The phylogenetic tree was

calculated using the MEGA application (Tamura et al., 2007) with the neighbor-joining method, with bootstrap values generated from 1,000 bootstrap samples. Only bootstrap values higher than 70% were considered to be significant (Hillis and Bull, 1993), and bootstrap values lower than 60% are not shown.

Plant Material and Plant Transformation

Arabidopsis (*Arabidopsis thaliana*) accession Col-0 and *qrt1* mutant seeds were obtained from the Arabidopsis Biological Resource Center (http://abrc.osu.edu/). T-DNA insertion mutants (*dcf-1*, Salk_040807; *dcf-2*, SAIL_513_C03) were localized in the SIGnAL Salk (http://signal.salk.edu/) and Syngenta (McElver et al., 2001) collections and obtained from the Arabidopsis Biological Resource Center. Plants were germinated and grown on soil (PRO-MIX; Premier Horticulture) in a growth chamber under short-day light conditions (10-h photoperiod [120 μmol m^{-2} s^{-1}] at 22°C and 60% relative humidity [RH]/14 h of dark at 22°C and 60% RH). After 4 weeks, plants were transferred to long-day conditions (16-h photoperiod [120 μmol m^{-2} s^{-1}] at 22°C and 60% RH/8 h of dark at 22°C and 60% RH). Arabidopsis plants were transformed using *Agrobacterium tumefaciens* GV 3101 pmp90 via the floral-dip method as described by Clough and Bent (1998). For BASTA selection, seeds were germinated on soil as described above and sprayed every 2 d for a total of five times with a glufosinate-ammonium (Crescent Chemical) solution (40 μg mL^{-1}). Resistant plants were transferred to new pots and further grown as described above.

Permeability and Pathogen Assays

Toluidine blue permeability assays on fully expanded rosette leaves were carried out according to Kurdyukov et al. (2006). Chlorophyll leaching experiments were done according to Lolle et al. (1998). In brief, two rosette leaves per sample (four samples per genotype) were immersed in 5 mL of 80% (v/v) ethanol in the dark. At the indicated time points, 200-μL aliquots were removed and chlorophyll content was determined by measuring the absorption at 664 and 647 nm. *Botrytis cinerea* pathoassays were carried out according to Manabe et al. (2011). For treatments with *Pseudomonas syringae*, fully expanded leaves were infiltrated with diluted suspensions of *P. syringae* DC3000 containing 10E-6 cells mL^{-1} in 10 mM $MgCl_2$. At least four leaves were harvested from each genotype at each time point, surface sterilized in 70% (v/v) ethanol, and the bacterial growth inside the leaves was enumerated after extraction of the bacteria by maceration of the leaves followed by direct counting of the colonies after growth in nutrient yeast glycerol (NYG) medium containing 25 μg mL^{-1} rifampicin for 2 d at 28°C. White cabbage butterfly (*Pieris rapae*) eggs were purchased from Carolina Biological Supply Company. Eggs were placed on radish (*Raphanus sativus*) plants, and 2 d after hatching, caterpillars of equal size were transferred to 8-week-old rosette-stage Arabidopsis plants grown under short-day conditions as described above and weighed after 7 d of feeding. Flea beetle (*Phyllotreta nemorum*) feeding experiments were carried out according to Nielsen et al. (2001).

Cloning Procedures

DCF (At3g48720) was cloned from cDNA prepared from Arabidopsis leaf RNA. The coding sequence without a native start or stop codon was PCR amplified using the following primer pairs: DCF-start$^+$-fwd (5′-CACCATGGTCGCCTCATCTGAGTT-3′)/DCF-stop$^-$-rev (5′-GATCTTCATAAGCTCTTCAAACACTT-3′) and DCF-start$^-$-fwd (5′-CACCGTCGCCTCATCTGAGTT-3′)/DCF-stop$^+$-rev (5′-TCAGATCTTCATAAGCTCTTCA-3′). The resulting PCR products were introduced into the pENTR SD/D TOPO cloning vector (Invitrogen) according to the manufacturer's protocol. Their identities were verified by sequencing. For expression under the control of the native promoter as C-terminal translational HA tag and YFP-HA tag fusions, the corresponding promoter sequence (2.49 kb upstream of the ATG start codon) was PCR amplified from genomic DNA with the *Not*I linker (lowercase letters) using DCF_{pro}-fwd (5′-ttgcggccgcaaAAAAGAAAACATAACCGAAGAGACGGTTT-3′) and DCF_{pro}-rev (5′-ttgcggccgcaaTTCAATGAAAGAAATCGAAAAACGTATGGA-3′). Following restriction digestion, the promoter sequence was ligated into the *Not*I site of the pENTR SD/D TOPO cloning vector upstream of the corresponding coding sequence. Orientation and identity were verified by sequencing. To obtain HA tag fusions, the construct was introduced into the promoterless pEarleyGate301 plant transformation vector (Earley et al., 2006) using LR Clonase (Invitrogen) according to the manufacturer's protocol. A C-terminal YFP-HA tag fusion construct was generated by replacing the *Nco*I/*Mun*I cassette from pEarleyGate301 by the *Nco*I/*Mun*I cassette derived from pEarleyGate101 (Earley et al., 2006). For heterologous expression in *Escherichia coli*, the coding sequence without the native start codon was recombined into the pDEST17 bacterial expression vector (Invitrogen), which introduces an N-terminal 6× His tag, using LR Clonase (Invitrogen) according to the manufacturer's protocol.

Heterologous Expression and Enzyme Purification

Each construct was introduced into BL-21 Star (DE3) chemically competent *E. coli* (Invitrogen) according to the manufacturer's instructions. A single bacterial colony, grown on Luria-Bertani agar containing 100 μg mL^{-1} carbenicillin, was isolated to inoculate a 5-mL liquid culture supplemented with 100 μg mL^{-1} carbenicillin and grown overnight at 37°C. The overnight culture was used to inoculate a 0.2-L Luria-Bertani culture containing 100 μg mL^{-1} carbenicillin, which was grown at 37°C until the optical density at 600 nm reached approximately 0.5. Expression was induced by the addition of 1 mM isopropyl-β-D-thiogalactopyranoside, and the culture was further grown at 20°C overnight. The recombinant protein was affinity purified using a HIS-Select HF Nickel Affinity Gel (Sigma-Aldrich) according to the manufacturer's instructions and desalted with PD-10 desalting columns (GE Healthcare). Purity and integrity were verified by SDS-PAGE, and the recombinant protein was stored at −20°C in 20 mM Tris buffer, pH 7.5, containing 20% (v/v) glycerol.

Hydroxycinnamoyl-CoA-Transferase Assay

If not otherwise indicated, transferase assays were performed at 50°C for 2 h in 50-μL reactions containing 50 mM Tris buffer, pH 7.5, 200 μM hydroxycinnamate-CoA, 1 μg of recombinant or 50 μg of total plant protein, and 1 mM acyl acceptor. The reactions were terminated by boiling for 10 min at 95°C. After the addition of 50 μL of methanol, reactions were subjected to HPLC. HPLC analysis was carried out using a Dionex Ultimate 3000 apparatus with UV detection. Samples were separated on a reverse-phase C18 column (Synergy 4u Fusion-RP 80A, 250 × 2.0 mm; Phenomenex). Prior to injection (20 μL), the samples were spin filtered (0.45 μm). A flow of 0.3 mL min^{-1} and a gradient of solvent A (0.2% [v/v] trifluoroacetic acid) and solvent B (acetonitrile) was applied as follows: 0 to 5 min, 10% B isocratic; 5 to 20 min, 10% to 100% B linear; 20 to 25 min, 100% B isocratic; 25 to 26 min, 100% to 10% B linear; 26 to 35 min, 10% B isocratic.

Extraction and HPLC Separation of Wall-Bound Phenolics

Frozen plant material was ground to a fine powder in liquid nitrogen, immersed in hot isopropanol, and extracted twice in isopropanol (85°C for 30 min) and for 2 h at room temperature. Soluble lipids were sequentially extracted with chloroform:methanol (2:1, v/v) for 2 h, chloroform:methanol (1:2, v/v) overnight, and methanol for 2 h. All steps were performed in 10-mL Teflon tubes at room temperature on a rocking agitator with 5 mL of solvent. Insoluble residues were vacuum dried for 24 h in a Speed-Vac at 30°C and subsequently used for lipid composition analysis or further processing. Total wall-bound phenolics were extracted by hydrolyzing about 20 mg of delipidated insoluble residue in 4 mL of 2 N sodium hydroxide at 22°C for 16 h. After acidification with 0.8 mL of concentrated hydrochloric acid, samples were extracted three times in ethyl acetate. The combined supernatants were dried under a stream of nitrogen and solubilized in 50% (v/v) methanol. Alternatively, prior to hydrolysis, pectins were removed by sequential extraction in 50 mM sodium phosphate, pH 7.1, 50 mM CDTA, and 50 mM sodium carbonate. Xylans were extracted from pectin-free residues with endo-β-xylanase and driselase (Sigma-Aldrich) as described elsewhere (Gou et al., 2009). Fractions were freeze dried and then separately hydrolyzed and extracted in ethyl acetate as described above. HPLC separation was done as described above with a gradient of solvent A (0.2% trifluoroacetic acid) and solvent B (acetonitrile) as follows: 0 to 5 min, 10% B isocratic; 5 to 25 min, 10% to 30% B linear; 25 to 40 min, 30% B isocratic; 40 to 45 min, 30% to 35% B linear; 45 to 46 min, 35% to 100% B linear; 46 to 51 min, 100% B isocratic; 51 to 53 min, 100% to 10% B linear; 53 to 60 min, 10% B isocratic. Statistical analyses were carried out using Student's *t* test.

Protein Extraction and Immunoblotting

Plant material was ground in liquid nitrogen. Soluble protein was extracted in 1 mL of 10 mM Tris, pH 7.5, 400 mM Suc, and 1 mM dithiothreitol. The resulting homogenate was thoroughly shaken for 20 min at 4°C, filtered through two layers of Miracloth, and centrifuged for 10 min at 1,500*g*. The resulting supernatant was centrifuged at 100,000*g* at 4°C for 60 min, and the supernatant (F1) containing predominantly cytosolic proteins was collected. To extract membrane and other residual proteins, the microsomal pellet was resuspended in 10 mM Tris, pH 7.5, 10% (v/v) glycerol, 1 mM dithiothreitol, and 0.5% (v/v) Triton X-100 and incubated for 30 min on ice. Protein concentrations were determined according to Bradford (1976). For immunoblot analysis, protein extracts were resolved by SDS-PAGE on 7% to 15% gradient gels and blotted onto nitrocellulose membranes (GE Healthcare). Blots were probed with a 1:1,000 dilution of rabbit anti-cFBPase (Agrisera; AS04 043) or anti-calreticulin (Abcam; ab2907) or a 1:10,000 dilution of rabbit anti-HA or mouse anti-poly-His antibody, respectively (Sigma-Aldrich), followed by a 1:20,000 dilution of goat anti-rabbit or goat anti-mouse IgG conjugated to horseradish peroxidase (Sigma-Aldrich),

Microscopy

Tissue samples were mounted in 10% (v/v) glycerol. Cells were plasmolyzed in 1 M potassium nitrate. Images were collected using a Leica MZ16F fluorescence stereomicroscope with 470 or 360 nm for GFP or UV light excitation, respectively. Confocal laser scanning microscopy was performed using a Zeiss LSM 710 equipped with an argon laser (514 nm for YFP excitation). Emission was collected at 510 to 545 nm. The pinhole diameter was set at 1 Airy unit. Images were processed in ImageJ 1.42q (http://rsb.info.nih.gov/ij) and Adobe Photoshop (Adobe Systems).

Determination of Lipid Composition

Insoluble residues were prepared as described above and subsequently depolymerized by acid-catalyzed transmethylation with methanolic hydrochloric acid essentially as described by Franke et al. (2005). In brief, acid-catalyzed transmethylation of insoluble residues (about 40 mg) was done by incubation for 2 h at 80°C in 2 mL of 3 N methanolic hydrochloric acid containing 10% (v/v) methyl acetate as cosolvent and 20 μg of methyl heptadecanoate as internal standard. After the addition of 1 mL of saturated sodium chloride/water, fatty acid methyl esters were extracted twice in dichloromethane. Phases were separated by centrifugation for 2 min at 1,500*g*. The organic phases were combined, washed with 2 mL of 0.9% (w/v) sodium chloride, dried over anhydrous sodium sulfate, and evaporated under a gentle stream of nitrogen gas. For GC-MS analysis, fatty acid methyl esters were derivatized for 15 min at 100°C in 0.1 mL of *N*,*O*-bis(trimethylsilyl)-trifluoroacetamide and 0.1 mL of pyridine, dried under a stream of nitrogen gas, and dissolved in ethyl acetate. GC-MS was carried out as described by Molina et al. (2006).

LC-APCI-MS

Liquid chromatographic separation was conducted on an Inertsil ODS-3 reverse-phase column (250 × 2.1 mm, 3-μm particle size; GL Sciences) using a 1200 HPLC system (Agilent). The injection volume was 2 μL. The sample tray and column compartment were maintained at 4°C and 55°C, respectively. The mobile phase was composed of water (solvent A) and methanol (solvent B). Analytes were separated at a flow of 0.25 mL min^{-1} with the following gradient: 0 to 5 min, 90% to 98% B linear; 5 to 25 min, 98% B isocratic; 25 to 32 min, 98% to 90% B linear; 32 to 40 min, 90% B isocratic. The HPLC system was coupled to an Agilent Technologies 6210 time-of-flight (TOF) mass spectrometer. Nitrogen gas set to 10 L min^{-1} and 30 ψ was used as nebulizing and drying gas. A drying gas temperature of 325°C was used throughout. The vaporizer and corona were set to 350°C and 4 μA, respectively. APCI was conducted with a capillary voltage of 3 kV. MS experiments were carried out in the full-scan mode (*m/z* 102–1,000) at 0.85 spectra s^{-1}. The instrument was tuned for a range of *m/z* of 50 to 1,700. Prior to LC-APCI-TOF MS analysis, the TOF MS device was calibrated with the Agilent APCI TOF tuning mix. Data acquisition and processing were performed by the MassHunter software package (Agilent).

RT-PCR

RNA was extracted using the RNEasy RNA Plant Kit (Qiagen) according to the manufacturer's protocol. One microgram of total RNA was reverse transcribed with SuperScript II reverse transcriptase and d(T)$_{15}$ oligomers (Invitrogen) according to the manufacturer's protocol. Real-time PCR was done with ABsolute SYBR Green ROX Mix (ABgene) on a StepOnePlus Real-Time PCR System (Applied Biosystems) according to the conditions described earlier (Czechowski et al., 2005) using StepOne 2.0 software (Applied Biosystems). *DCF* was amplified using primers 5′-CCGGTAGTAGTTCAGGTGACAA-3′ (forward) and 5′-GGGACGGATAAAGGAAGACC-3′ (forward). As a reference, primers for *UBQ10* (5′-GGCCTTGTATAATCCCTGATGAATAAG-3′ [forward] and 5′-AAAGAGATAACAGGAACGGAAACATAGT-3′ [forward]) were used.

Supplemental Data

The following materials are available in the online version of this article.

Supplemental Figure S1. Chlorophyll extraction from rosette leaves.

Supplemental Figure S2. Susceptibility of *dcf* mutants to fungal and bacterial pathogens.

Supplemental Figure S3. Susceptibility of *dcf* mutants to herbivores.

Supplemental Figure S4. Pairwise alignment of HHT/ASFT and DCF full-length amino acid sequences.

Supplemental Figure S5. Bootstrapped neighbor-joining tree of the Arabidopsis BAHD gene family of acyl-CoA-dependent acyl-transferases.

ACKNOWLEDGMENTS

Ms. Sherry Chan from the Joint BioEnergy Institute, Feedstocks Division, is thanked for assistance with plant growth. We thank Dr. Jens Kvist Nielsen from the University of Copenhagen, Department of Agriculture and Ecology, for the flea beetle experiments.

Received September 13, 2011; accepted December 7, 2011; published December 8, 2011.

LITERATURE CITED

Alonso JM, Stepanova AN, Leisse TJ, Kim CJ, Chen H, Shinn P, Stevenson DK, Zimmerman J, Barajas P, Cheuk R, et al (2003) Genome-wide insertional mutagenesis of *Arabidopsis thaliana*. Science **301:** 653–657

Altschul SF, Gish W, Miller W, Myers EW, Lipman DJ (1990) Basic local alignment search tool. J Mol Biol **215:** 403–410

Baker EA, Martin JT (1963) Cutin of plant cuticles. Nature **199:** 1268–1270

Bessire M, Chassot C, Jacquat AC, Humphry M, Borel S, Petétot JM, Métraux JP, Nawrath C (2007) A permeable cuticle in Arabidopsis leads to a strong resistance to Botrytis cinerea. EMBO J **26:** 2158–2168

Bradford MM (1976) A rapid and sensitive method for the quantitation of microgram quantities of protein utilizing the principle of protein-dye binding. Anal Biochem **72:** 248–254

Christensen A, Svensson K, Thelin L, Zhang W, Tintor N, Prins D, Funke N, Michalak M, Schulze-Lefert P, Saijo Y, Sommarin M, Widell S, Persson S (2010) Higher plant calreticulins have acquired specialized functions in Arabidopsis. PLoS One **5:** e11342

Clough SJ, Bent AF (1998) Floral dip: a simplified method for *Agrobacterium*-mediated transformation of *Arabidopsis thaliana*. Plant J **16:** 735–743

Czechowski T, Stitt M, Altmann T, Udvardi MK, Scheible WR (2005) Genome-wide identification and testing of superior reference genes for transcript normalization in Arabidopsis. Plant Physiol **139:** 5–17

D'Auria JC, Chen F, Pichersky E (2002) Characterization of an acyltransferase capable of synthesizing benzylbenzoate and other volatile esters in flowers and damaged leaves of *Clarkia breweri*. Plant Physiol **130:** 466–476

D'Auria JC, Pichersky E, Schaub A, Hansel A, Gershenzon J (2007a) Characterization of a BAHD acyltransferase responsible for producing the green leaf volatile (Z)-3-hexen-1-yl acetate in Arabidopsis thaliana. Plant J **49:** 194–207

D'Auria JC, Reichelt M, Luck K, Svatos A, Gershenzon J (2007b) Identification and characterization of the BAHD acyltransferase malonyl CoA:anthocyanidin 5-O-glucoside-6″-O-malonyltransferase (At5MAT) in Arabidopsis thaliana. FEBS Lett **581:** 872–878

Dudareva N, Pichersky E (2000) Biochemical and molecular genetic aspects of floral scents. Plant Physiol **122:** 627–633

Earley KW, Haag JR, Pontes O, Opper K, Juehne T, Song K, Pikaard CS (2006) Gateway-compatible vectors for plant functional genomics and proteomics. Plant J **45:** 616–629

Franke R, Briesen I, Wojciechowski T, Faust A, Yephremov A, Nawrath C, Schreiber L (2005) Apoplastic polyesters in Arabidopsis surface tissues: a typical suberin and a particular cutin. Phytochemistry **66:** 2643–2658

Gou JY, Yu XH, Liu CJ (2009) A hydroxycinnamoyltransferase responsible for synthesizing suberin aromatics in Arabidopsis. Proc Natl Acad Sci USA **106:** 18855–18860

Hillis D, Bull J (1993) An empirical test of bootstrapping as a method for assessing confidence in phylogenetic trees. Syst Biol **42:** 182–192

Jia XY, He LH, Jing RL, Li RZ (2009) Calreticulin: conserved protein and diverse functions in plants. Physiol Plant **136:** 127–138

Kolattukudy PE (1980) Biopolyester membranes of plants: cutin and suberin. Science **208:** 990–1000

Kolattukudy PE (2001) Polyesters in higher plants. Adv Biochem Eng Biotechnol **71:** 1–49

Kurdyukov S, Faust A, Nawrath C, Bär S, Voisin D, Efremova N, Franke R, Schreiber L, Saedler H, Métraux JP, et al (2006) The epidermis-specific extracellular BODYGUARD controls cuticle development and morphogenesis in *Arabidopsis*. Plant Cell **18:** 321–339

Li Y, Beisson F, Koo AJ, Molina I, Pollard M, Ohlrogge J (2007) Identification of acyltransferases required for cutin biosynthesis and production of cutin with suberin-like monomers. Proc Natl Acad Sci USA **104:** 18339–18344

Lotfy S, Javelle F, Negrel J (1996) Purification and characterization of hydroxycinnamoyl-coenzyme A:ω-hydroxypalmitic acid O-hydroxycinnamoyltransferase from tobacco (*Nicotiana tabacum* L.) cell-suspension cultures. Planta **199:** 475–480

Lotfy S, Negrel J, Javelle F (1994) Formation of omega-feruloyloxypalmitic acid by an enzyme from wound-healing potato tuber discs. Phytochemistry **35:** 1419–1424

Lolle SJ, Hsu W, Pruitt RE (1998) Genetic analysis of organ fusion in *Arabidopsis thaliana*. Genetics **149:** 607–619

Luo J, Fuell C, Parr A, Hill L, Bailey P, Elliott K, Fairhurst SA, Martin C, Michael AJ (2009) A novel polyamine acyltransferase responsible for the accumulation of spermidine conjugates in *Arabidopsis* seed. Plant Cell **21:** 318–333

Luo J, Nishiyama Y, Fuell C, Taguchi G, Elliott K, Hill L, Tanaka Y, Kitayama M, Yamazaki M, Bailey P, et al (2007) Convergent evolution in the BAHD family of acyl transferases: identification and characterization of anthocyanin acyl transferases from *Arabidopsis thaliana*. Plant J **50:** 678–695

Ma X, Koepke J, Panjikar S, Fritzsch G, Stöckigt J (2005) Crystal structure of vinorine synthase, the first representative of the BAHD superfamily. J Biol Chem **280:** 13576–13583

Manabe Y, Nafisi M, Verhertbruggen Y, Orfila C, Gille S, Rautengarten C, Cherk C, Marcus SE, Somerville S, Pauly M, et al (2011) Loss-of-function mutation of REDUCED WALL ACETYLATION2 in Arabidopsis leads to reduced cell wall acetylation and increased resistance to *Botrytis cinerea*. Plant Physiol **155:** 1068–1078

McElver J, Tzafrir I, Aux G, Rogers R, Ashby C, Smith K, Thomas C, Schetter A, Zhou Q, Cushman MA, et al (2001) Insertional mutagenesis of genes required for seed development in *Arabidopsis thaliana*. Genetics **159:** 1751–1763

Molina I, Bonaventure G, Ohlrogge J, Pollard M (2006) The lipid polyester composition of Arabidopsis thaliana and Brassica napus seeds. Phytochemistry **67:** 2597–2610

Molina I, Li-Beisson Y, Beisson F, Ohlrogge JB, Pollard M (2009) Identification of an Arabidopsis feruloyl-coenzyme A transferase required for suberin synthesis. Plant Physiol **151:** 1317–1328

Nielsen JK, Hansen ML, Agerbirk N, Petersen BL, Halkier BA (2001) Responses of the flea beetles *Phyllotreta nemorum* and *P. cruciferae* to metabolically engineered *Arabidopsis thaliana* with an altered glucosinolate profile. Chemoecology **11:** 75–83

Panikashvili D, Shi JX, Schreiber L, Aharoni A (2009) The Arabidopsis DCR encoding a soluble BAHD acyltransferase is required for cutin polyester formation and seed hydration properties. Plant Physiol **151:** 1773–1789

Pollard M, Beisson F, Li Y, Ohlrogge JB (2008) Building lipid barriers: biosynthesis of cutin and suberin. Trends Plant Sci **13:** 236–246

Ranathunge K, Schreiber L, Franke R (2011) Suberin research in the genomics era: new interest for an old polymer. Plant Sci **180:** 399–413

Rani SH, Krishna TH, Saha S, Negi AS, Rajasekharan R (2010) Defective in cuticular ridges (DCR) of *Arabidopsis thaliana*, a gene associated with surface cutin formation, encodes a soluble diacylglycerol acyltransferase. J Biol Chem **285:** 38337–38347

Rautengarten C, Baidoo E, Keasling JD, Scheller HV (2010) A simple method for enzymatic synthesis of unlabeled and radiolabeled hydroxycinnamate-CoA. Bioenerg Res **3:** 115–122

Reina-Pinto JJ, Yephremov A (2009) Surface lipids and plant defenses. Plant Physiol Biochem **47:** 540–549

Samuels L, Kunst L, Jetter R (2008) Sealing plant surfaces: cuticular wax formation by epidermal cells. Annu Rev Plant Biol **59:** 683–707

Schmid M, Davison TS, Henz SR, Pape UJ, Demar M, Vingron M, Schölkopf B, Weigel D, Lohmann JU (2005) A gene expression map of Arabidopsis thaliana development. Nat Genet **37:** 501–506

Schreiber L (2010) Transport barriers made of cutin, suberin and associated waxes. Trends Plant Sci **15:** 546–553

Sieber P, Schorderet M, Ryser U, Buchala A, Kolattukudy P, Métraux JP, Nawrath C (2000) Transgenic *Arabidopsis* plants expressing a fungal cutinase show alterations in the structure and properties of the cuticle and postgenital organ fusions. Plant Cell **12:** 721–738

Strand A, Zrenner R, Trevanion S, Stitt M, Gustafsson P, Gardeström P (2000) Decreased expression of two key enzymes in the sucrose biosynthesis pathway, cytosolic fructose-1,6-bisphosphatase and sucrose phosphate synthase, has remarkably different consequences for photosynthetic carbon metabolism in transgenic *Arabidopsis thaliana*. Plant J **23:** 759–770

Suh MC, Samuels AL, Jetter R, Kunst L, Pollard M, Ohlrogge J, Beisson F (2005) Cuticular lipid composition, surface structure, and gene expression in Arabidopsis stem epidermis. Plant Physiol **139:** 1649–1665

Suzuki H, Nakayama T, Yonekura-Sakakibara K, Fukui Y, Nakamura N, Nakao M, Tanaka Y, Yamaguchi MA, Kusumi T, Nishino T (2001) Malonyl-CoA:anthocyanin 5-O-glucoside-6″-O-malonyltransferase from scarlet sage (Salvia splendens) flowers: enzyme purification, gene cloning, expression, and characterization. J Biol Chem **276:** 49013–49019

Taguchi G, Ubukata T, Nozue H, Kobayashi Y, Takahi M, Yamamoto H, Hayashida N. (2010) Malonylation is a key reaction in the metabolism of xenobiotic phenolic glucosides in Arabidopsis and tobacco. Plant J **63:** 1031–1041

Tamura K, Dudley J, Nei M, Kumar S (2007) MEGA4: Molecular Evolutionary Genetics Analysis (MEGA) software version 4.0. Mol Biol Evol **24:** 1596–1599

Thompson JD, Gibson TJ, Plewniak F, Jeanmougin F, Higgins DG (1997) The CLUSTAL_X Windows interface: flexible strategies for multiple sequence alignment aided by quality analysis tools. Nucleic Acids Res **25:** 4876–4882

Winter D, Vinegar B, Nahal H, Ammar R, Wilson GV, Provart NJ (2007) An "Electronic Fluorescent Pictograph" browser for exploring and analyzing large-scale biological data sets. PLoS ONE **2:** e718

Yu XH, Chen MH, Liu CJ (2008) Nucleocytoplasmic-localized acyltransferases catalyze the malonylation of 7-O-glycosidic (iso)flavones in Medicago truncatula. Plant J **55:** 382–396

Yu XH, Gou JY, Liu CJ (2009) BAHD superfamily of acyl-CoA dependent acyltransferases in Populus and Arabidopsis: bioinformatics and gene expression. Plant Mol Biol **70:** 421–442